THE INCIDENCE ANGLES OF THE TRACKERS USED FOR THE PV PANELS' ORIENTATION. PART II: AZIMUTHAL TRACKERS

Ion VIŞA, Dorin DIACONESCU, Valentina DINICU, Bogdan BURDUHOS
"Transilvania" University of Braşov, Romania

Abstract. Firstly, this second part of the paper models and simulates the azimuthal PV tracker incidence angle variations. On the basis of the numerical simulations, there are presented a comparative analysis of the incidence angle variations obtained with the two tracker types (azimuthal and pseudoequatorial) and the main conclusions derived from this analysis. The results are very useful in the tracker's design.

1. Introduction

The main objective of this second part of the paper is to model the azimuthal PV tracker incidence angle. In order to do this, firstly the paper establishes the sun-ray unit vector and the PV panel normal unit vector; by means of these unit vectors, there is modelled the incidence angle. Secondly, there are made some simulations for this modelling. The simulations' results enable the comparative analysis of the azimuthal dual-axis tracker versus the (pseudo)equatorial dual-axis tracker and the horizontally fixed, respectively titled fixed solar panels cases.

In the figure 1 there are illustrated the Earth- tracker relative position and the due angles of the azimuthal system $Qx_0y_0z_0$ (ψ, α).

2. Unit vectors modelling

For energetic and economical reasons, the angular displacement of the tracked PV panel is made discontinuously (in steps), so the tracker's angles ψ and α have discreet variations. In order to distinguish them from the sun-ray angles (which have continuous variations: ψ and α; see figure 1) in the below correlations the tracker's angles are marked with asterisk: ψ^* and α^* (see figures 2 and 3).

From figure 1, which shows the sunray geometry in the local system $Qx_0y_0z_0$, the following expression of the sunray unit vector can be obtained:

$$[\bar{e}_{sr}]_{x_oy_oz_o} = \begin{bmatrix} \cos\alpha \cdot \sin\psi \\ -\cos\alpha \cdot \cos\psi \\ \sin\alpha \end{bmatrix}. \qquad (1)$$

Figure 2 illustrates the kinematical scheme of the azimuthal dual-axis tracker, in which interfere three reference systems: the local system X0Y0Z0 and two intermediate systems $X_1Y_1Z_1$ and $X_2Y_2Z_2$; the unit vector of the axis Z_2 is perpendicular on the PV panel. From figure 2 the following correlation of the PV panel normal unit vector can be established:
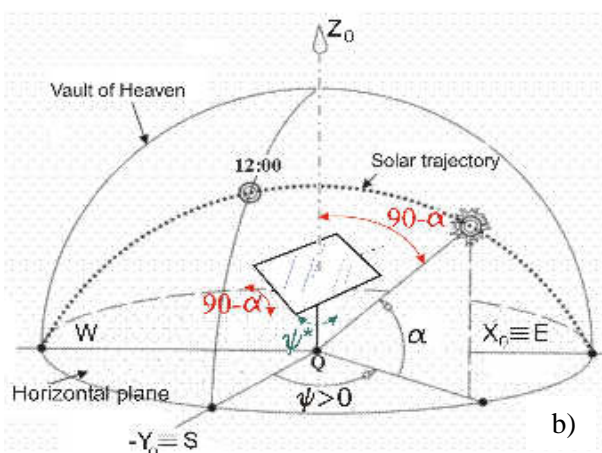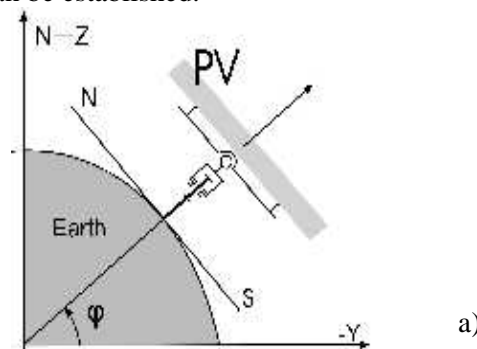

a)

b)

Figure 1. The scheme of the azimuthal PV tracker related to:
a) the Earth and b) the observer reference system

$$\overline{e}_{PV-az} = [k_2]_{x_0 y_0 z_0} = T_{1 \to 0} \cdot T_{2 \to 1} \cdot [k_2]_2 =$$

$$= \begin{bmatrix} \cos\psi^* & -\sin\psi^* & 0 \\ \sin\psi^* & \cos\psi^* & 0 \\ 0 & 0 & 1 \end{bmatrix} \cdot$$

$$\cdot \begin{bmatrix} 1 & 0 & 0 \\ 0 & \cos(90-\alpha^*) & -\sin(90-\alpha^*) \\ 0 & \sin(90-\alpha^*) & \cos(90-\alpha^*) \end{bmatrix} \begin{bmatrix} 0 \\ 0 \\ 1 \end{bmatrix} =$$

$$= \begin{bmatrix} \sin\psi^* \cos\alpha^* \\ -\cos\psi^* \cdot \cos\alpha^* \\ \sin\alpha^* \end{bmatrix}_{x_0 y_0 z_0} \quad (2)$$
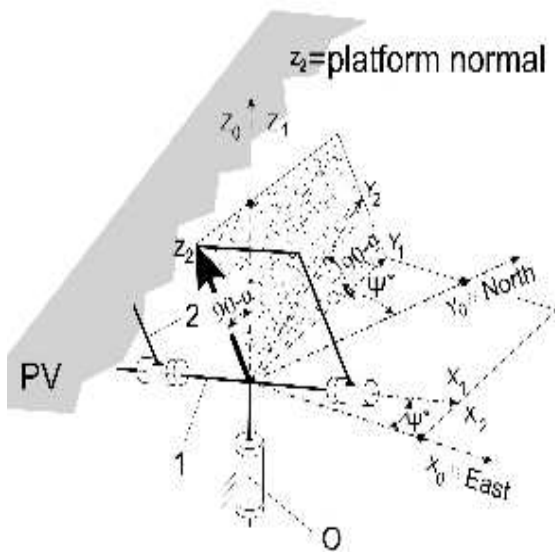
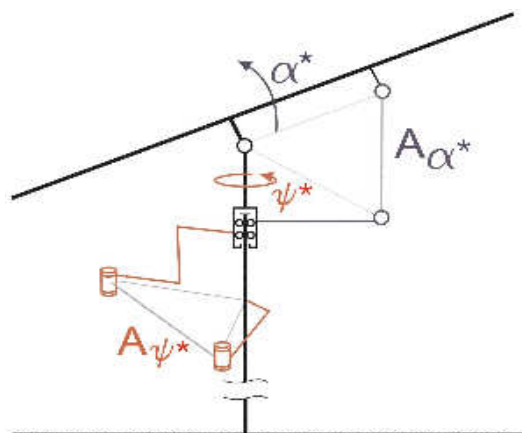Figure 2. Kinematical scheme of the azimuthal dual-axis tracker

Figure 3. The scheme of the tracker's actuators

Figure 3 illustrates the scheme of the azimuthal tracker with its linear actuators A_ψ and A_α; these actuators drive the tracker's angular displacements ψ^* and α^*.

3. Sunray-PV panel incidence angle

The incidence angle between the sunray and the PV panel, orientated by the azimuthal tracker, can be obtained using the correlations (1) and (2):

$$\cos\nu = \overline{e}_{sun-ray} \cdot \overline{e}_{PV-az} =$$

$$= \begin{bmatrix} \cos\alpha \cdot \sin\psi \\ -\cos\alpha \cdot \cos\psi \\ \sin\alpha \end{bmatrix} \cdot \begin{bmatrix} \sin\psi^* \cos\alpha^* \\ -\cos\psi^* \cdot \cos\alpha^* \\ \sin\alpha^* \end{bmatrix} = \quad (3)$$

$$= \cos\alpha \cdot \sin\psi \cdot \cos\alpha^* \cdot \sin\psi^* +$$
$$+ \cos\alpha \cdot \cos\psi \cdot \cos\alpha^* \cdot \cos\psi^* + \sin\alpha \cdot \sin\alpha^*$$

4. Numerical simulations and interpretation

Using the incidence angle model, depicted by the realation (3), some numerical simulations were made, by means of the Excel software. In these simulations were considering the following input data: a) latitude $\varphi = 45°$ N, b) day $n = 172$ Summer Solstice (June 21st) $\Leftrightarrow \delta = +23.45°$, c) day $n = 355$ Winter Solstice (December 21st) $\Leftrightarrow \delta = -23.45°$ and d) days $n = 80$ and 262 Spring Equinox (March 21st), respectively Autumn Equinox (October 21st) $\Leftrightarrow \delta = 0°$.

An orientation cycle of the solar panel consists in: aprox. 1 min. displacement + aprox. 59 min. standing.

The simulations' results are illustrated in figures $4 \div 18$.

Figures 4, 5, 9, 10, 14, 15 illustrate that the incidence angles of an azimuthal dual-axis tracker have smaller variation compared with the ones of an equatorial dual-axis tracker ; the incidence angles variation of the equatorial dual-axis tracker is bigger in the morning and in the evening. On the other side, the ignitions number and the acting time of the motors are smaller in the equatorial tracker case.

The figures 6, 7, 11, 12, 16, 17 illustrate that the azimuthal displacement has a much higher influence on the tracking accuracy than the altitudinal displacement.

As it can be seen in figures 5, 7, 10, 12, 15, 17, the azimuthal tracker, with $\alpha^* \approx 40° =$ constant, achieves incidence angles' variations comparable to the equatorial tracker variations.

In the considered numerical situation (see figures 6, 8, 11, 13, 16, 18), the incidence angles' variations of the fixed PV panels are about similar between them and net bigger than the tracked panels.
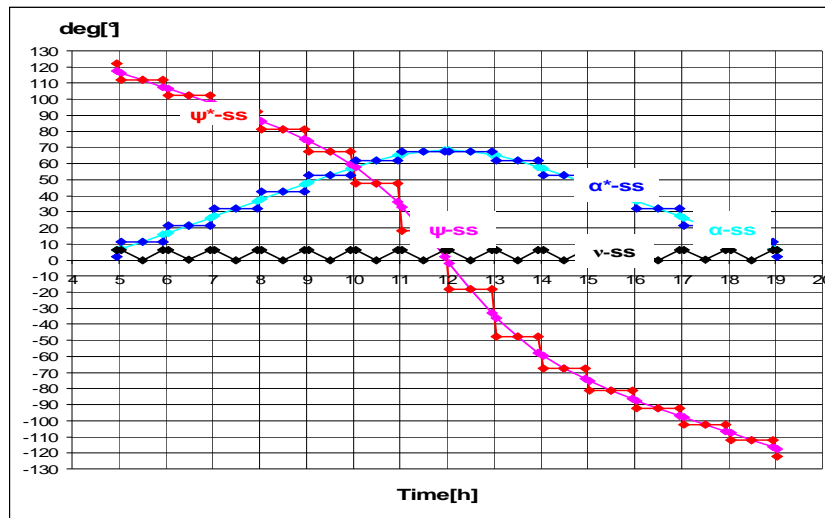
Figure 4. The incidence and auxiliary angles variations of the azimuthal dual-axis tracker, during the *summer solstice*.
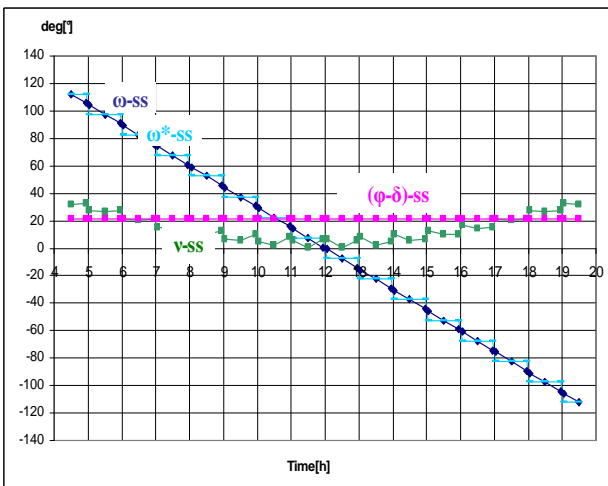

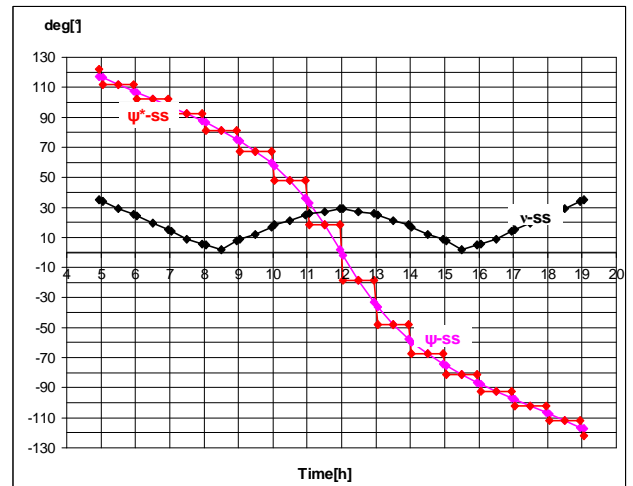Figure 5. Summer solstice variations for the (pseudo)equatorial dual-axis tracker

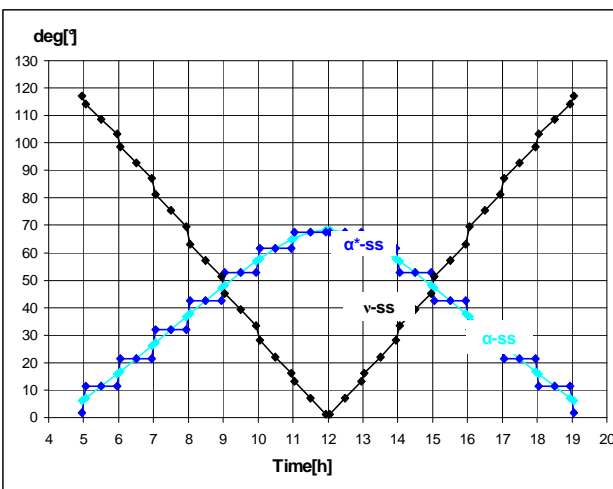Figure7. Summer solstice ν variation for an azimuthal single-axis tracker with α* = 40

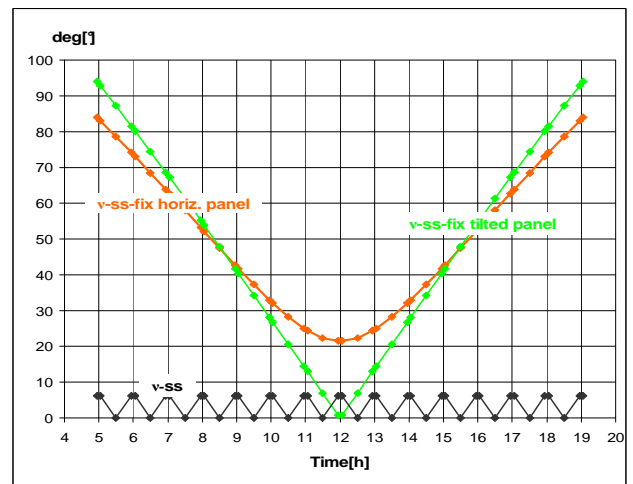Figure 6. Summer solstice *ν* variation for an azimuthal single-axis tracker with ψ* = 0

Figure 8. Summer solstice variation of the incidence angle ν for the azimuthal dual-axis tracker vs. horizontally fixed and tilted fixed panels
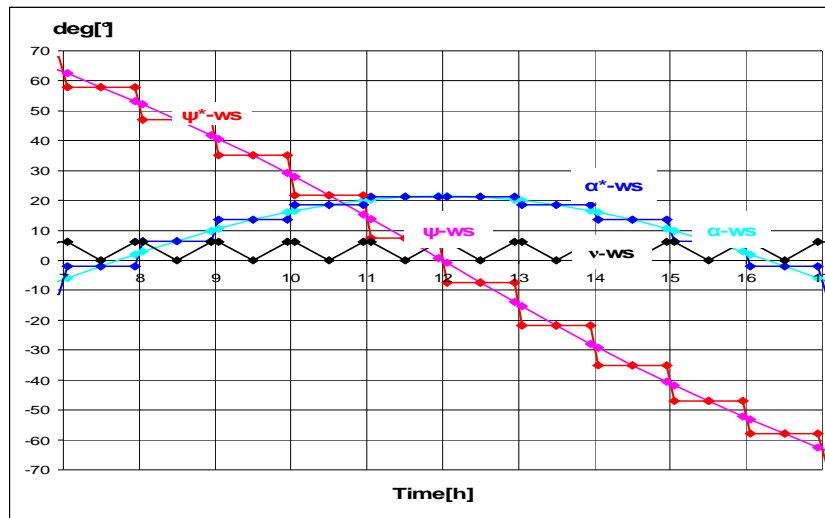
Figure 9. The incidence and auxiliary angles variations of the azimuthal dual-axis tracker, during the winter solstice
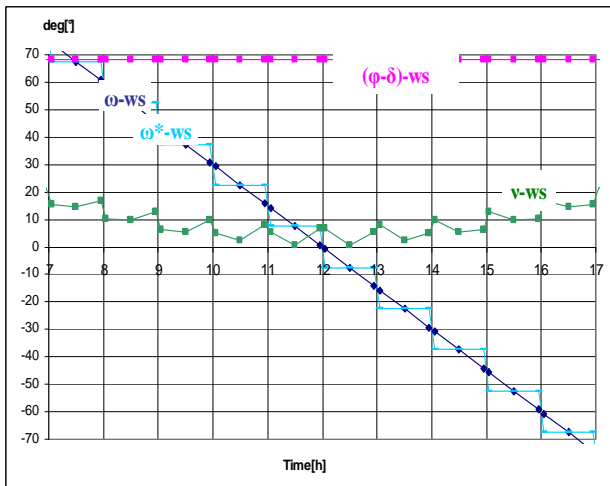

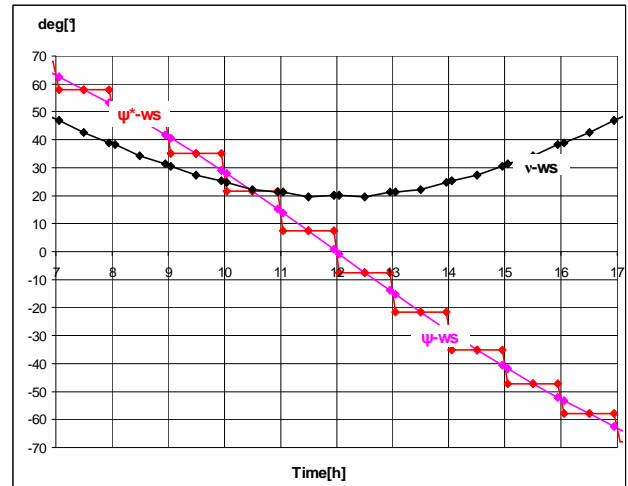Figure 10. Winter solstice for the (pseudo)equatorial dual-axis tracker

Figure 12. Winter solstice ν variation for an azimuthal single-axis tracker with α* = 40
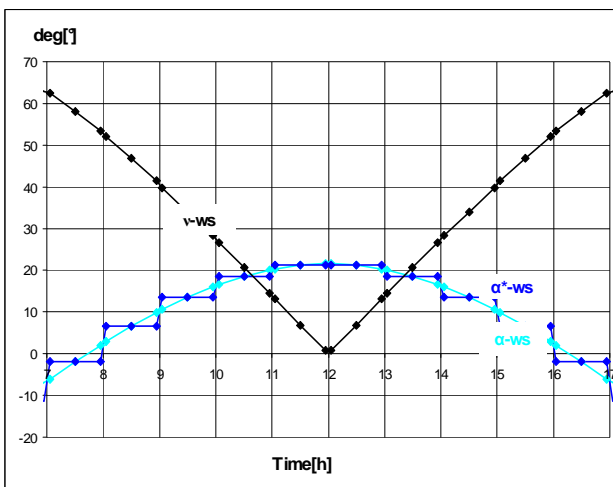

Figure 11. Winter solstice ν variation for an azimuthal single-axis tracker with ψ* = 0
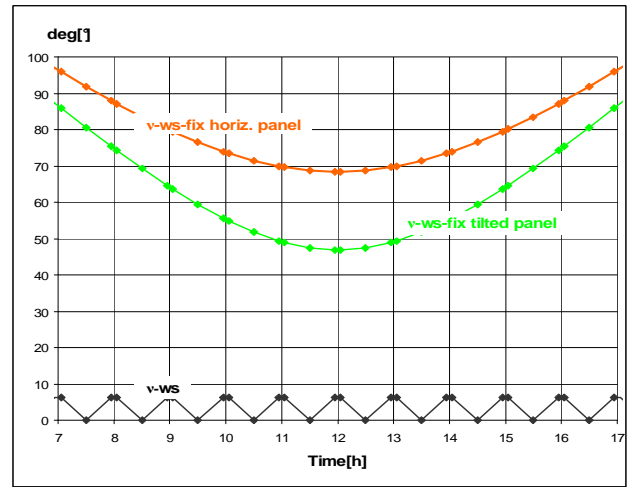

Figure 13. Winter solstice variation of the incidence angle ν for the azimuthal dual-axis tracker vs. a horizontally fixed and a tilted fixed panels
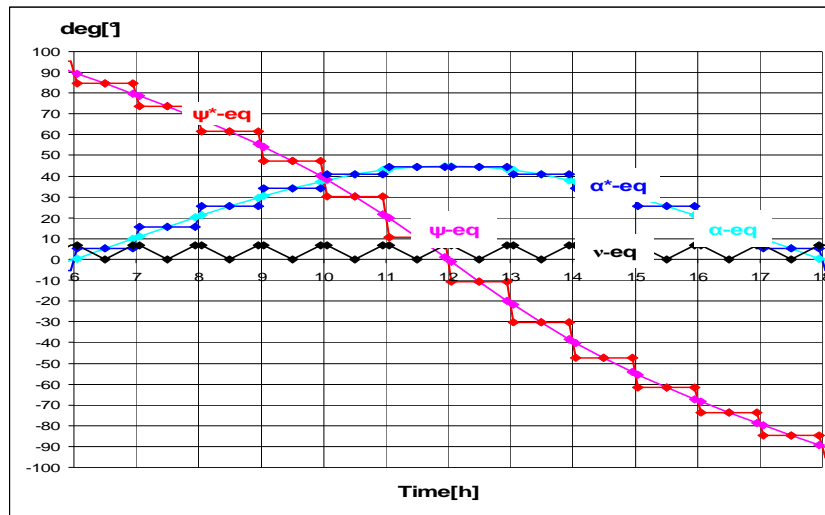
Figure 14. The incidence and auxiliary angles variations of the azimuthal dual-axis tracker, during the equinoxes
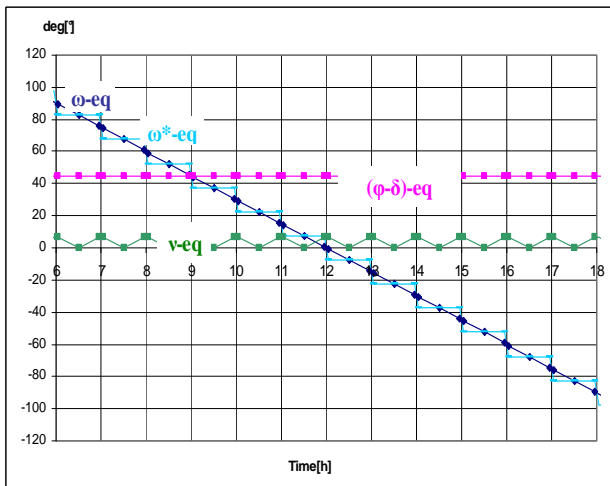

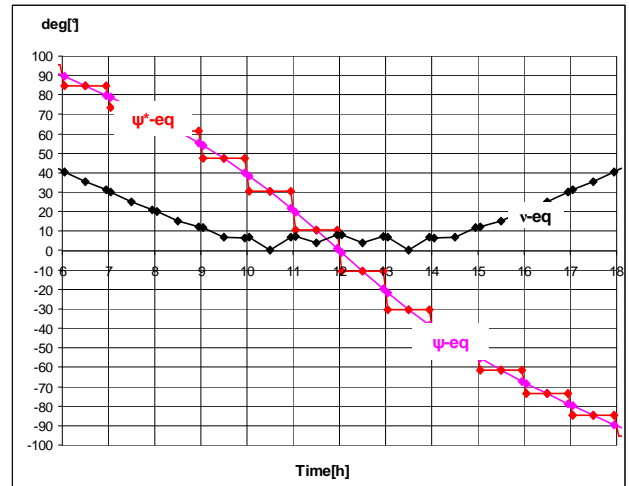Figure 15. Equinoxes variations for the (pseudo)equatorial dual-axis tracker

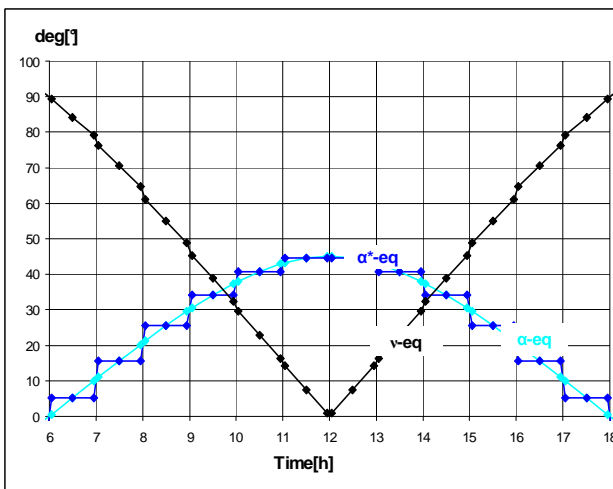Figure 17. Equinoxes variations for an azimuthal single-axis tracker with α* = 40

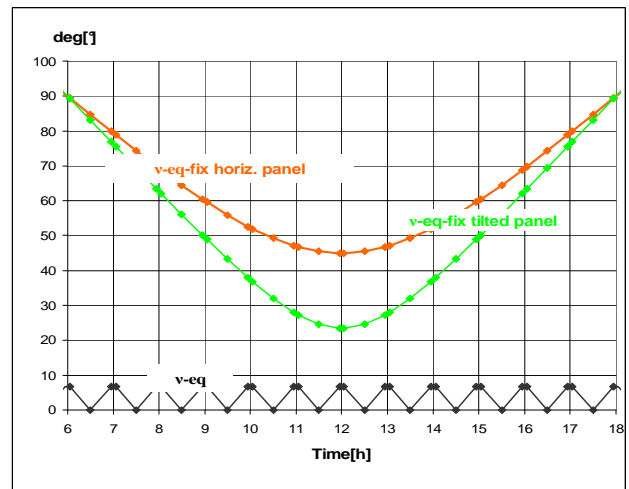Figure 16. Equinoxes variations for an azimuthal single-axis tracker with ψ* = 0

Figure 18. Equinoxes variation of the incidence angle ν for the azimuthal dual-axis tracker vs. a horizontally fixed and a tilted fixed panels

5. Conclusions

In this second part of the paper there was modelled the incidence angle for the azimuthal dual-axis PV tracker.

The model was tested with Excel software using numerical simulations.

The comparison between the dual-axis azimuthal tracker and dual-axis (pseudo) equatorial tracker highlights that:

the dual-axis equatorial tracker achieve bigger incidence angle variation, but this tracker achieves also a smaller motor ignitions number and a smaller acting time (that is a smaller energetic consumption).

The numerical simulations have shown that the azimuthal displacement of an azimuthal tracker has a higher influence on the tracking accuracy than the altitudinal displacement.

The significant difference between the incidence angle of a tracked panel and the one of a horizontally fixed or tilted fixed panel emphasizes the fact that the panel tracking is efficient and recommendable to be used in practice.

References

1. Messenger, R., Ventre, J.: *Photovoltaic System Engineering*, London, CRC Press, 2000, ISBN 0-8493-1793-2.
2. Diaconescu, D. a.o.: Analysis of the Sun-Earth angles used in the design of the solar collectors' trackers, Bulletin of the Transilvania University of Brasov, Vol.13(47), ISBN 1223-9631, 2006, pp. 99-105.
3. Goswami, D.J., Kreith, K., Kreider, J.F.: *Principles of Solar Engineering,* Philadelphia, PA, George H. Buchanan Co., 1999, .ISBN 978-1560327141.
4. Meliss, M.,: *Regenerative Energy Sources*, Springer-Verlag, Berlin Heidelberg, 1997, ISBN 978-0387550855 (in German).
5. Stine, B.W., Harrigan, R.W.: *Solar Energy Fundamentals and Design*, West Sussex, USA, John Wiley & Sons, 1985, ISBN 0471887188.